ISR Spectra Estimates via Higher-Order Stochastic Modeling of Coulomb Collisions

BRIAN LA ROSA[1], DAVID HYSELL[1], MARCO MILLA[2]

Cornell University [1], Pontific Catholic University of Peru [2]

EQUIT-03

bl639@cornell.edu

1. BACKGROUND

- The ISR technique yields estimates of plasma density, temperature, and composition by fitting experimental backscattered signals to theoretical plasma models. The resulting ISR spectrum is expressed as:

ISR Spectrum:

$$\langle |n_e(\mathbf{k},\omega)|^2\rangle = \frac{|1+\chi_i|^2}{|1+\chi_i+\chi_e|^2}\langle |n_{te}(\mathbf{k},\omega)|^2\rangle + \frac{|\chi_e|^2}{|1+\chi_i+\chi_e|^2}\langle |n_{ti}(\mathbf{k},\omega)|^2\rangle$$

where

$$\langle |n_{ts}(\mathbf{k},\omega)|^2\rangle = 2n_s Re\{J_s(\omega)\} \qquad J_s(\omega) = \int_0^{\infty} e^{-i\omega\tau}\langle e^{i\mathbf{k}\cdot\Delta\mathbf{r}_s(\tau)}\rangle d\tau$$

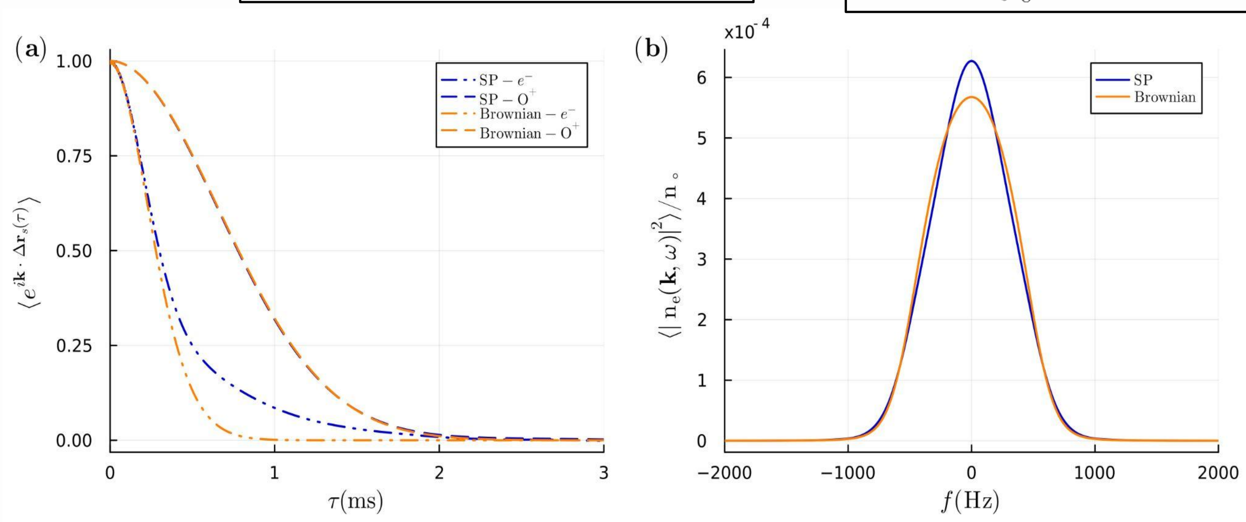

Figure 1: Simulation of a) the electron and ion characteristic functions, employed to compute (b) the net ISR spectrum, for a O+ plasma using the following parameters: Te, Ti=1000K and ne=1e12 m3, aspect angle α=1.0° and λr=6 m.

- Accurate spectrum reproduction requires accounting for Coulomb collisions at small magnetic aspect angles (<6°).
- This work enhances the single particle (SP) scheme of Milla and Kudeki (2011) by implementing higher-order stochastic differential equation (SDE) solvers.

2. FOKKER-PLANCK AND LANGEVIN EQUATION EQUIVALENCE

- **Challenge:** While the Fokker-Planck equation provide the complex stochastic description of the collisional processes, it is computationally demanding.
- **Approach:** Instead an equivalent Langevin equation formulation is used for a more efficient mathematical treatment.

Fokker-Planck Equation:

$$\frac{\partial f_s}{\partial t} = -\frac{\partial}{\partial \mathbf{v}}\left[A(\mathbf{v},t)f_s(\mathbf{v},t)\right] + \frac{1}{2}\frac{\partial^2}{\partial\mathbf{v}\partial\mathbf{v}} : \left[D(\mathbf{v},t)f_s(\mathbf{v},t)\right]$$

Complementary perspectives of the same physical process.

Langevin Equation:

$$d\mathbf{v} = \mathbf{A}(\mathbf{v},t)dt + \mathbf{D}^{1/2}(\mathbf{v},t)dW(t) + \underbrace{\frac{q_s}{m_s}\mathbf{v}\times\mathbf{B}_o dt}_{\text{Gyromotion}}$$

- The physics of these collisional interactions is fully determined by the friction (*A*) and diffusion (*D*) coefficients. Table 1 summarizes different models:

Particle Dynamics	A(v,t)	D(v,t)	B field
Collisional	ν	$\frac{2KT\nu}{m}$	-
Magnetized	-	-	☑
Brownian	ν	$\frac{2KT\nu}{m}$	☑
Coulomb Collisions	$\sum_{s'}\Gamma_{ss'}\nabla_{\mathbf{v}}H(\mathbf{v}_s)$	$\sum_{s'}\Gamma_{ss'}\frac{\mu_{ss'}}{m_s}\nabla_{\mathbf{v}}\nabla_{\mathbf{v}}G(\mathbf{v}_s)$	☑

Table 1: Particle dynamics approximations with corresponding friction (*A*), diffusion (*D*), and magnetic field terms. With ν as the collision frequency; *H(v)* and *G(v)* denote the first and second Rosenbluth potentials (Bellan, 2006).

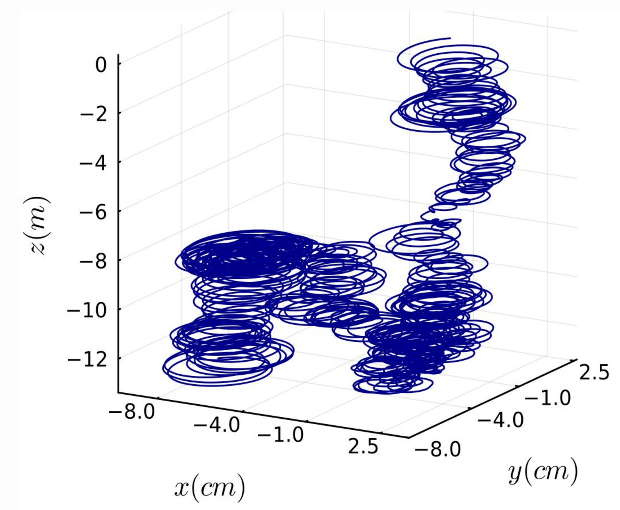

Figure 2: A 400 us simulated electron trajectory undergoing friction, diffusion and gyromotion effects.

- We solve the Langevin equation under a Coulomb collision approximation to obtain the particle displacements (Δr) required for the ISR spectrum (Figure 1).

3. WEAK CONVERGENCE ANALYSIS

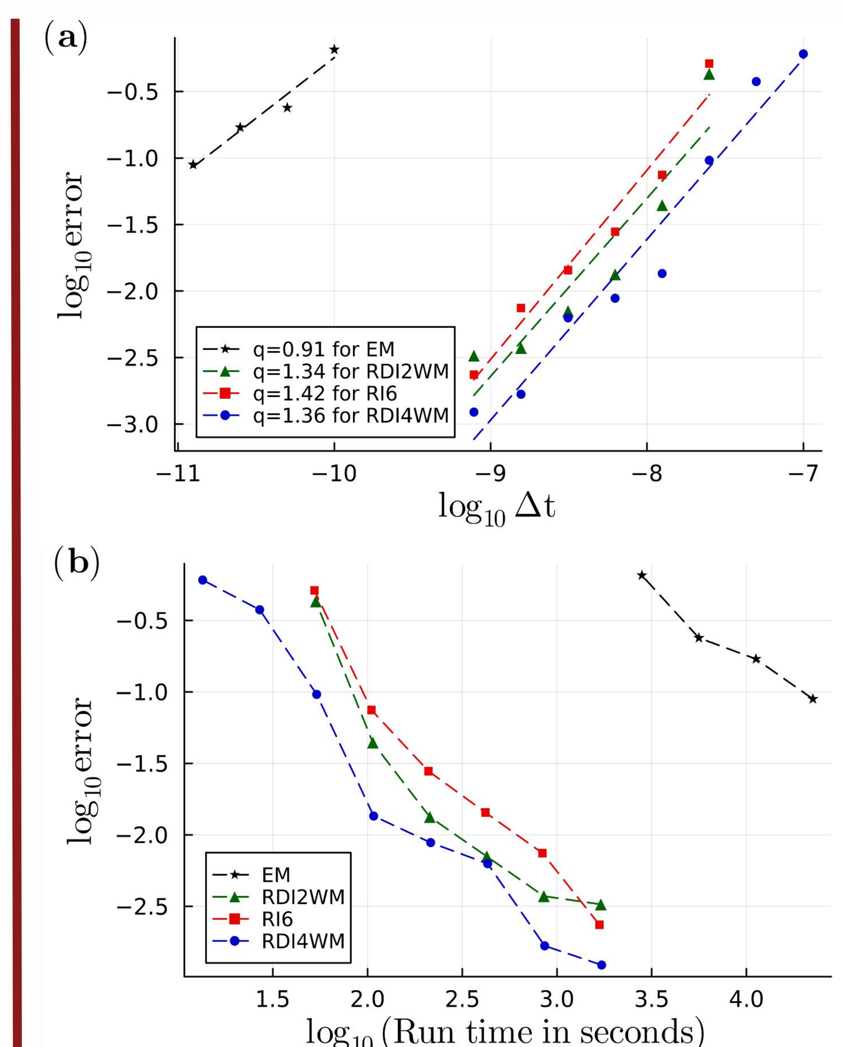

Figure 3: (a) Convergence order and (b) computational efficiency versus precision for SDE solvers modeling the electron Langevin equation (N = 1e5 independent Monte Carlo samples).

- The previously stated Langevin equation with velocity-dependent coefficients can only be solved numerically.
- Using DifferentialEquations.jl in Julia language, we benchmarked higher-order SDE solvers against the standard Euler-Maruyama approach via a weak convergence test (Figure 3a).

Weak Order of Convergence:

$$|E[g(X(t_f))] - E[g(\tilde{X}(t_f))]| \leq C\Delta t^q$$

Estimator:

$$E[g(\tilde{\mathbf{v}}(t_f))] = \frac{1}{N}\sum_{i=1}^{N}\frac{1}{2}mv_i^2(t_f)$$

True Value:

$$E[g(\mathbf{v})] = \frac{3}{2}kT.$$

- As shown in Figure 3, the **RDI4WM algorithm** provides the optimal balance of efficiency and precision among the candidates, effectively mitigating the computational limitation imposed by the stiff Langevin equation.

4. TIME DISCRETIZATION ANALYSIS

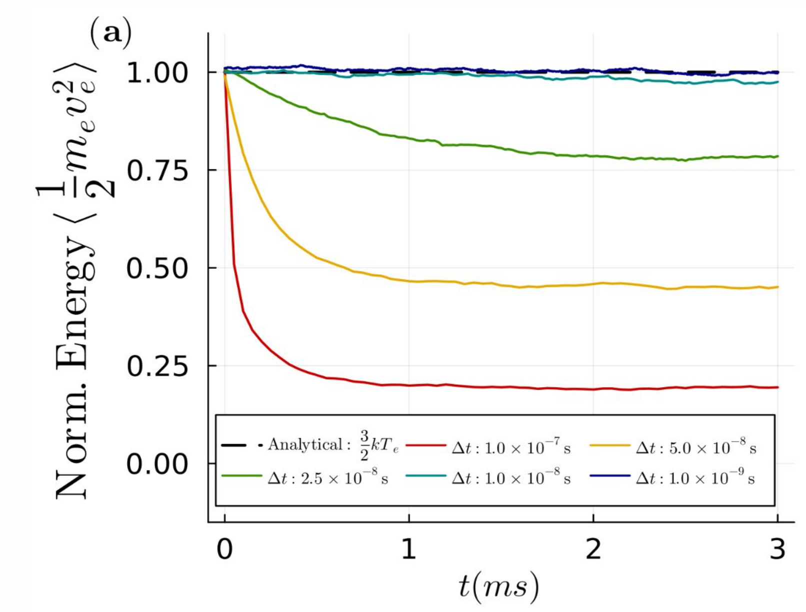

Figure 4: Temporal evolution of the mean particle electron energy from a pre-thermalized initialization using the RDI4WM solver.

- While the RDI4WM scheme remains stable, larger time steps can introduce a numerical bias in the steady-state energy.
- Figure 4 reveals the time-step dependence required to achieve the correct thermalized energy.

Optimal Δt resolution → Thermalized Energy $\frac{3}{2}kT$

- Consequently, the electron characteristic function exhibits clear sensitivity to temporal discretization (Figure 5).

$$\langle e^{i\mathbf{k}\cdot\Delta\mathbf{r}(m\Delta t)}\rangle = \frac{1}{N}\sum_{n=1}^{N}\frac{1}{M-m}\sum_{j=1}^{M-m} e^{i\mathbf{k}\cdot(\mathbf{r}_n(j+m)-\mathbf{r}_n(j))}$$

- It converges numerically for Δt<1e-8 s, with no appreciable improvement at finer resolutions.

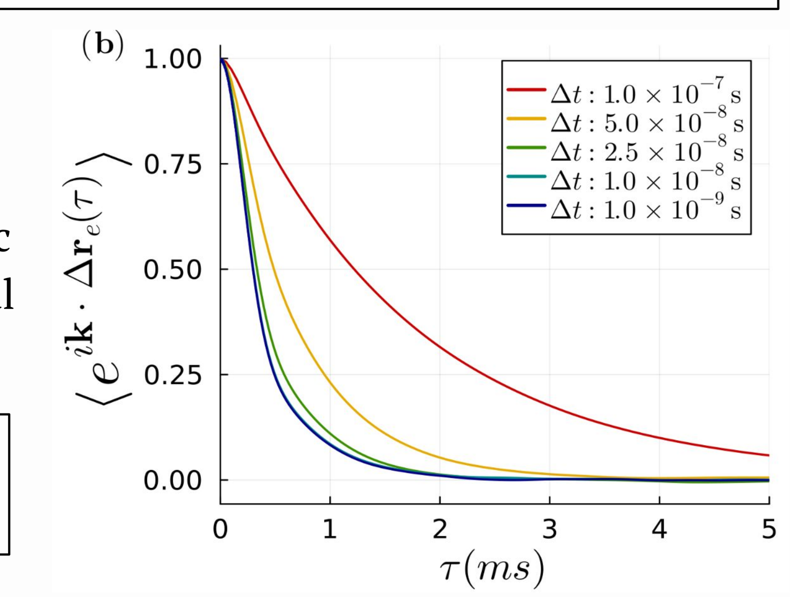

Figure 5 : Electron characteristic function computed using λr=6 m. and an aspect angle of α=1.0° for different time discretizations.

5. RESULTS: ISR/ACF LIBRARY INCLUDING COULOMB COLLISIONS

- A complete ISR/ACF library was numerically computed by applying the optimized RDI4WM scheme to the Coulomb-collisional Langevin framework (see Table 2).
- Rather than storing massive particle trajectory data, the solver directly computes and saves the characteristic function.

Parameters	Range
Temperature (T_s)	600: 200: 4000 K
Density (n_s)	10^(10 : 0.5 :13) m^{-3}
Magnetic field (B_o)	15: 5 : 25 μT
Aspect Angle (α)	{0.0, 0.01, 0.05, 0.1}° & 0.5: 0.5: 6.0 °

Table 2: Range of plasma parameters included in the ISR/ACF library. All possible permutations of this parameters are included.

Simulation Parameters:

- Trajectories: 1000
- Δt: 1e-8
- Final time: 100 ms
- Threads: 32

Performance:

- Exe. Time = 5 min
- Mem. Allocation: ~15 Gb Ram

Diagram 1: Simulation parameters and performance metrics per plasma configuration

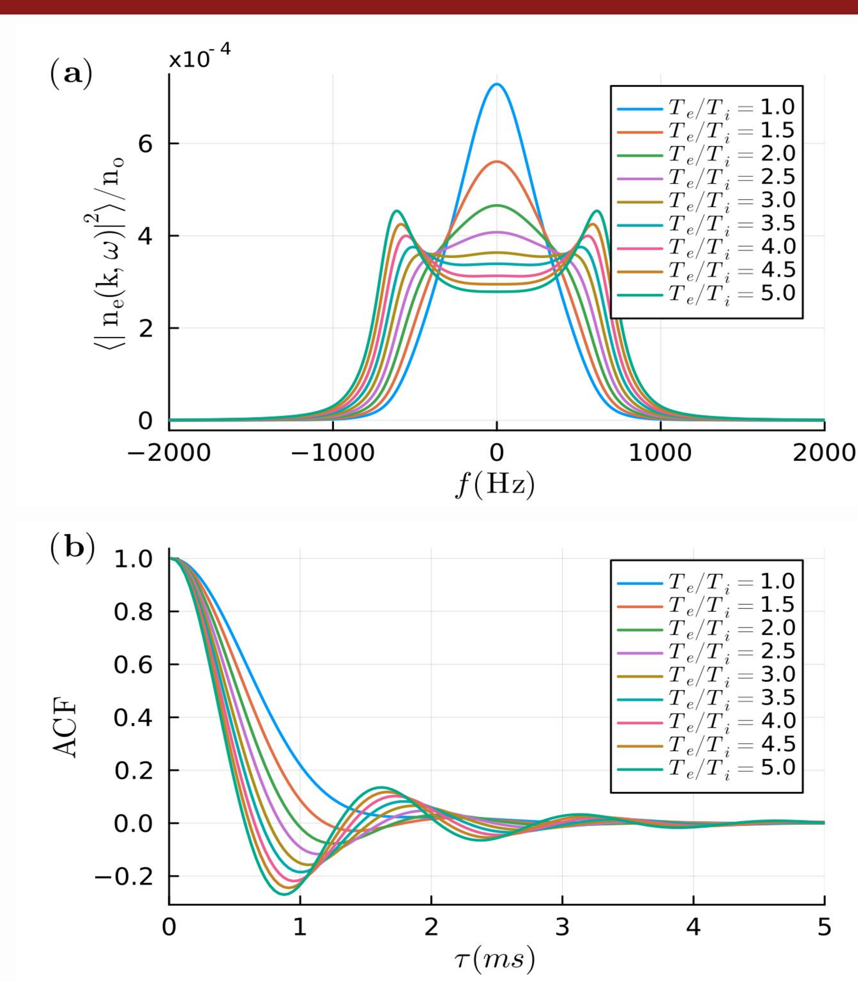

Figure 6 : (a) ISR spectrum and (b) ACF for different temperature ratios. Parameters: Ne=1e12, α=1.0°, B=25uT and Ti=800 K.

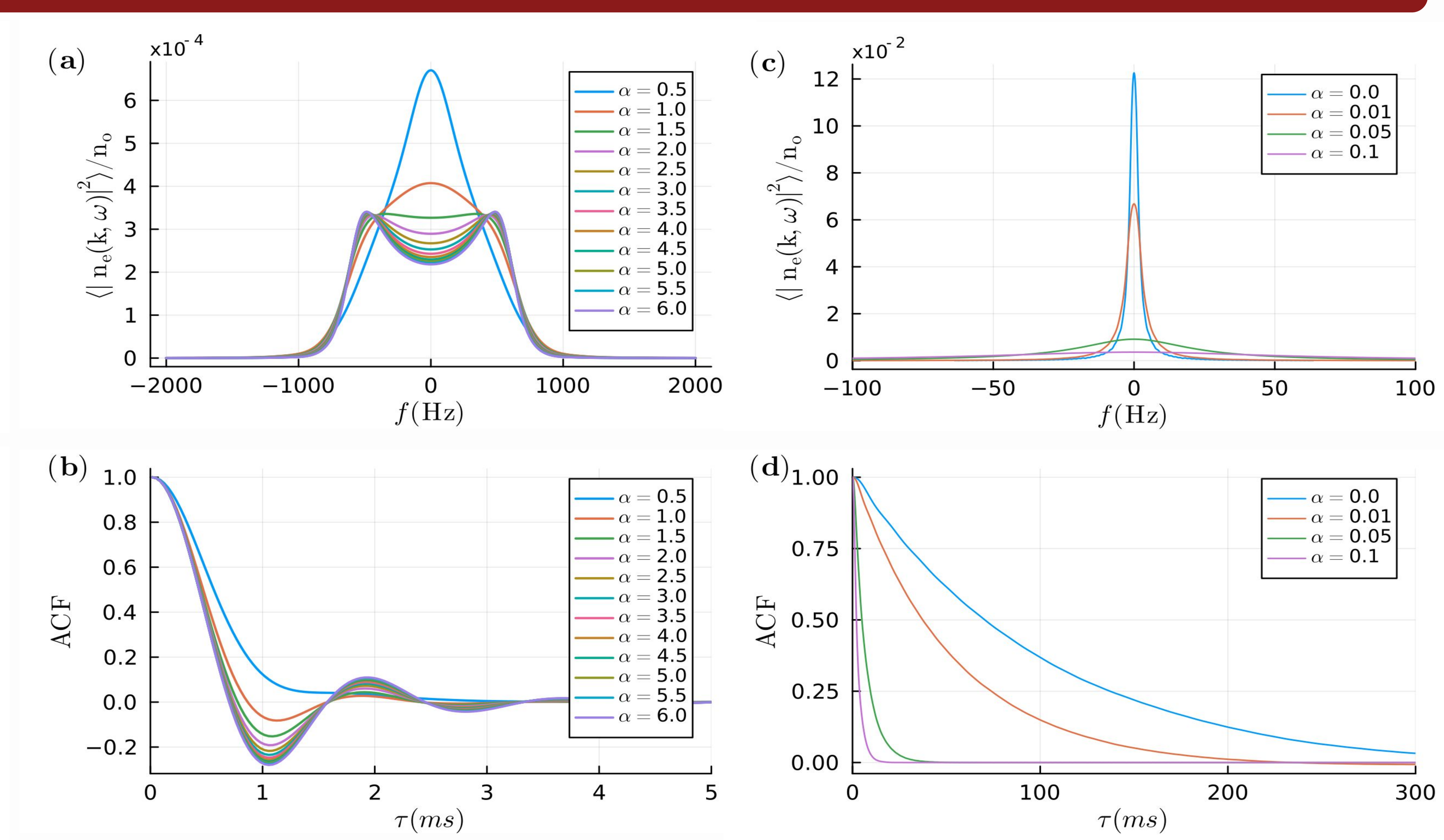

Figure 7: (a,c) ISR spectrum and (b,d) ACF for different magnetic aspect angles. Parameters: Ne=1e11, B=25uT, Te=2000 K and Ti=1000 K.

- Each plasma configuration was simulated using the baseline parameters defined in Diagram 1, where the corresponding solver performance is also detailed. However, the final time was extended to 1s for the smaller aspect angles.
- Figures 6 and 7 illustrate the dependence of the ISR spectra and ACFs on temperature and magnetic aspect angle across various plasma configurations. Here, the extension of the final time for smaller aspect angles is evident (Figure 7d).

6. CONCLUSIONS

- Implementing the higher-order SDE solver RDI4WM accurately captures electron dynamics while outperforming standard algorithms. Additionally, we reduce computational complexity by using a fixed time step Δt=1e-8 s.
- We present a comprehensive numerical library of ISR spectra and ACF profiles including the effects of Coulomb collisions. This library covers an extensive parameter space of ionospheric plasma configurations. Implemented entirely within an open-source Julia language ecosystem, this framework provides a highly reproducible foundation for validating collisional plasma models.
- In the future, parameter space will be expanded using ML techniques and validated against real experimental data.

7. REFERENCES

[1] Kudeki, E. & Milla, M.A. (2011). IEEE Transactions on Geoscience and Remote. Incoherent scatter spectral theories-Part II: A general result for small magnetic as Sensing, vol 49, pp 315-328. doi: 10.1109/TGRS.2010.2057252

[2] Rackauckas, Christopher and Nie, Qing (2017). The Journal of Open Research Software. A Performant and Feature-Rich Ecosystem for Solving Differential Equations in Julia Vol 5. doi:10.5334/jors.151

[3] Bellan, P. (2006). Fundamentals of plasma physics. Cambridge University Press.